catalysts

MDPI

Article

ZIF-8 Metal Organic Framework for the Conversion of Glucose to Fructose and 5-Hydroxymethyl Furfural

Ryan Oozeerally [1], Shivendra D. K. Ramkhelawan [1,2], David L. Burnett [3], Christiaan H. L. Tempelman [2] and Volkan Degirmenci [1,*]

1 School of Engineering, University of Warwick, Coventry CV4 7AL, UK; R.Oozeerally@warwick.ac.uk (R.O.); shivendraramkhelawan@gmail.com (S.D.K.R.)
2 Department of Chemical Engineering, Rotterdam University of Applied Sciences, Rotterdam Mainport Institute, Rotterdam 3024 EA, The Netherlands; c.h.l.tempelman@hr.nl
3 School of Metallurgy and Materials, University of Birmingham, Birmingham B15 2TT, UK; d.burnett@bham.ac.uk
* Correspondence: v.degirmenci@warwick.ac.uk; Tel.: +44-2476523385

Received: 3 September 2019; Accepted: 24 September 2019; Published: 27 September 2019

Abstract: Herein, Zeolitic imidazolate framework-8 (ZIF-8) is considered as an easy and cheap to prepare alternative catalyst for the isomerization of glucose and production of 5-hydroxymethyl furfural (HMF). For the synthesis of the ZIF-8 catalysts two preparation methods were evaluated, being room temperature and hydrothermal synthesis at 140 °C. Of these, the hydrothermal synthesis method yields a material with exceptionally high surface area (1967 $m^2 \cdot g^{-1}$). As a catalyst, the ZIF-8 materials generated excellent fructose yields. Specifically, ZIF-8 prepared by hydrothermal synthesis yielded a fructose selectivity of 65% with a glucose conversion of 24% at 100 °C in aqueous reaction medium. However, this selectivity dropped dramatically when the reactions were repeated at higher temperatures (~140 °C). Interestingly, greater quantities of mannose were produced at higher temperatures too. The lack of strong Brønsted acidity in both ZIF-8 materials resulted in poor HMF yields. In order to improve HMF yields, reactions were performed at a lower pH of 1.0. At 140 °C the lower pH was found to drive the reaction towards HMF and double its yield. Despite the excellent performance of ZIF-8 catalysts in batch reactions, their activity did not translate well to the flow reactor over a continuous run of 8 h, which was operating with a residence time of 6 min. The activity of ZIF-8 halved in the flow reactor at 100 °C in ~3 h, which implies that the catalyst's stability was not maintained in the long run.

Keywords: metal organic framework; zeolitic imidazolate framework; HMF; biomass; catalysis; glucose

1. Introduction

The conversion of biomass derived sugars into platform molecules has been studied extensively during the last decade [1,2]. This route has the potential to bridge the gap between a renewable resource, biomass, and the fuels and chemicals that our society needs. Among the current platform molecules, 5-hydroxymethyl furfural (HMF) is versatile and therefore has been considered as a promising building block for chemical industries in the context of sustainable development. Glucose is the most abundant sugar in biomass, and its conversion into HMF is attracting much attention [3]. One of the challenges of this transformation is to find a cheap catalyst that can be manufactured industrially. Another challenge is that the conversion leads to various side reactions, leading to by-products, which are poorly characterised polymeric species commonly referred as humins [4]. Therefore, finding a catalyst that is simple to synthesize and scalable, which can catalyse the conversion of glucose with high selectivity towards HMF is essential.

A landmark work for this research area is the discovery of Chromium (Cr) chloride catalysts in ionic liquid solvents [5]. Lewis acid Cr ions coordinated with the cations of the ionic liquid enables the isomerisation of glucose into fructose that leads to HMF yield of above 65%. The proton network surrounding the Cr ions together with the transient formation of bimetallic Cr active sides facilitate the hydride shift on the carbon atoms of glucose which is a key feature of this transformation [6]. This leads to the isomerisation of glucose into fructose which later converts into HMF, where the HMF selectivity is determined by the glucose isomerisation into fructose. In other words, the isomerisation of glucose into fructose was found to be the key step. The Lewis acid Cr sites provides the selectivity for glucose isomerisation, whereas the Brønsted acidity enhances the conversion rates. We also showed that a similar reaction mechanism is prevalent when other metal ions, such as iron (Fe) and Copper (Cu) are used [7,8]. A similar reaction environment can be replicated on the surface of a heterogeneous catalyst [9,10] which is more desirable than a homogeneous catalyst as industrial production is concerned. Scheme 1 shows the most common reaction pathways that have been proposed in the literature [11–13]. The isomerisation of glucose to fructose proceeds over a Lewis acid catalyst, and mannose can be produced as a by-product through epimerisation. The dehydration of fructose to 5-HMF is catalysed by Brønsted acids. Humins are insoluble carbon-rich materials that may also be formed as a by-product. These humins are adsorbed at the catalyst surface thereby causing the deactivation of the catalyst. One of the main contributor to the formation of humins is the highly reactive fructose as the reaction intermediate [14]. Another possible route for the formation of humins are mainly through the self-condensation of HMF and cross-polymerization of HMF with glucose or fructose.

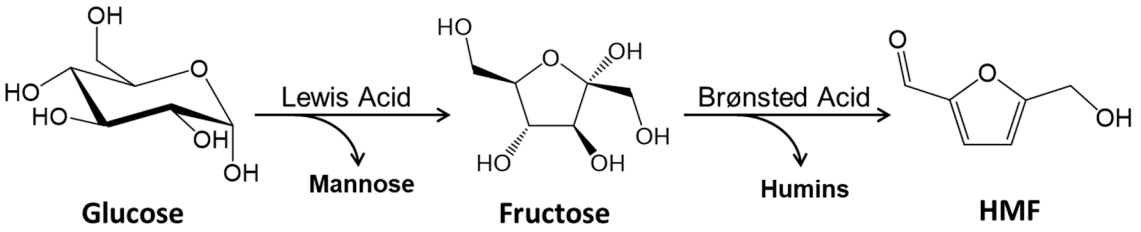

Scheme 1. Simplified reaction scheme for glucose conversion.

The heterogeneous Lewis acid Sn-Beta zeolites were reported to catalyse the glucose isomerization into fructose in water selectively [11,12,15]. The catalyst has isolated Lewis acid centres in a relatively hydrophobic molecular framework of zeolite Beta. It is anticipated that the intrinsic hydrophobicity of the beta zeolite surface plays an important role of limiting the excessive diffusion of water in micropores [16]. Furthermore, it facilitates the selective adsorption of less hydrophilic glucose and quick removal of fructose to aqueous phase, which prevents its further conversion into undesired side products [17,18]. It is clear that the local environment around Lewis acid (Sn) sites and hydroxyl density of zeolite framework at the surface is crucial for activity and selectivity in this reaction [19,20].

MIL-101 which has Cr as the metal in its framework is known to catalyse glucose conversion as well as fructose conversion to HMF [21]. We have recently reported a metal organic framework (MOF) heterogeneous catalyst—MIL-88B with iron (Fe) and Scandium (Sc) metals in its framework [22] for glucose to HMF conversion. Cr is not a desirable metal because of its acute toxicity. Therefore, we replaced the Cr of the MIL-101 framework with Fe and Sc metals. The extended synthesis times and high Sc inclusion lead to the formation of another MOF, namely MIL-88B which catalyses the reaction in dimethyl sulfoxide (DMSO) with an HMF selectivity of 70% at 35% glucose conversion. The synthesis procedure of MIL-88B (Fe, Sc) is tedious and difficult to control. A physical mixture of different MOFs, i.e. MIL-88B and MIL-101 forms with a slight variation in the synthesis protocol, which are the standing challenges to overcome for this type of MOF. Another MOF type catalyst that we have reported for glucose isomerisation and HMF production is UiO-66 [23]. The low coordinated zirconium sites on the surface of the UiO-66 provides Lewis acid sites. But the framework lacks Brønsted acidity.

Therefore, we partially replaced the linker, benzene dicarboxylic acid (BDC) in the UiO-66 MOF with 2-monosulfo-benzene-1,4-dicarboxylate (MSBDC). The addition of the sulfonic acid groups through this organic linker provided the required Brønsted acidity and the catalysts showed fructose and HMF yields of 22% and 6%, respectively with glucose conversion of 31%.

Our search for a MOF with a simple synthesis procedure brought our attention to Zeolitic imidazolate framework-8 (ZIF-8). It is one of the few commercially available MOFs that can be produced in continuous flow which addresses the challenges related to scale-up [24]. ZIF-8 contains 2-methylimidazolate linkers and zinc (Zn) metal ions arranged in a sodalite zeolite (SOD) type framework [25,26]. ZIF-8 exhibits high surface area, porosity, excellent thermal stability, and excellent chemical stability, which finds applications in catalysis, gas capture/separation, drug delivery, water treatment, and electrical energy storage [27–31]. For the application as a catalyst in the glucose to HMF conversion, the material contains the acidic bifunctionality. Namely, the Lewis acidity originating from framework incorporated Zn metals and the Brønsted acidity generated by the N-H groups of the imidazole organic linker. Although metals, Cr and Sn, have been the subject of many studies in the conversion of glucose into HMF, Zn has not been studied extensively. Zn did not indeed exhibit more remarkable performance for HMF production than above metals in the liquid phase, however, it is the choice of metal for a variety of catalytic reactions which requires Lewis acidity due to its outstanding performance [32,33]. Therefore, it is worthy of investigation for HMF production. Furthermore, the ZIF-8 material possess basic sites due to N- moieties and hydroxyl groups present in the material [26]. This has potential to provide a relatively hydrophobic framework similar to Sn-Beta zeolite catalyst.

In this work, we show that ZIF-8 can catalyse glucose conversion into HMF with an apparent production of fructose. This proves that ZIF-8 is an active catalyst for the isomerisation of glucose into fructose. Reactions were initially conducted in water–the most environmentally benign solvent–at two different temperatures (100 °C and 140 °C). Subsequently, in an attempt to increase the HMF production, reactions were also conducted at pH = 1.0. Finally, the performance of a ZIF-8 catalyst was tested in a continuous flow reactor.

2. Results and Discussion

2.1. Characterisation of Catalysts

The successful synthesis of ZIF-8 catalysts were confirmed by XRD analysis. Figure 1A shows the XRD pattern of the simulated pattern from literature [25] and ZIF-8 and ZIF-8-HT materials. A comparison of the catalysts with the simulated diffraction pattern shows a perfect match of the diffraction peaks. All diffraction peak positions of ZIF-8 and ZIF-8-HT are well matched with those of the simulation data, confirming that the products are crystalline ZIF-8. There are no additional peaks within the XRD pattern of ZIF-8 and ZIF-8-HT materials which proves that the materials do not contain uncoordinated organic linker. The absence of reflections of large zinc chloride particles indicates that zinc is well coordinated with the linker and stays in the metal organic framework. The sharp peaks of ZIF-8 and ZIF-8-HT indicates their high crystallinity. The full width half maximum values obtained from the major diffraction peak at 7.3° are 0.13°, 0.20°, and 0.14° for the reference spectra, ZIF-8, and ZIF-8-HT (Table 1). This shows that the crystallinity of the ZIF-8-HT catalyst is higher than the ZIF-8 material, and it is close to the reference pattern obtained from single crystal studies. The difference is due to the synthesis conditions. The synthesis of ZIF-8-HT was performed at higher temperature and pressure in autoclaves. During the hydrothermal synthesis crystallization occurred from high-temperature aqueous synthesis solution at high vapour pressures, which resulted in highly crystalline catalyst. Confirmation of the identity and crystallinity of MOF structure is provided by a more detailed analysis of higher resolution powder X-ray diffraction patterns, and Figure 1B,C show the profile fits to the ZIF-8 and ZIF-8-HT materials, respectively. The refined lattice parameters fitted using the cubic space-group I-43m are consistent with those reported in the literature [34] for

ZIF-8 materials from experimental data of X-ray diffraction [35] and neutron powder diffraction [36]. For example, Liedana et al. [37] found a = 17.084 Å and V = 4986.19 Å^3, and Haldoupis et al. [38] reported a = 17.137 Å, which are in agreement with our findings.

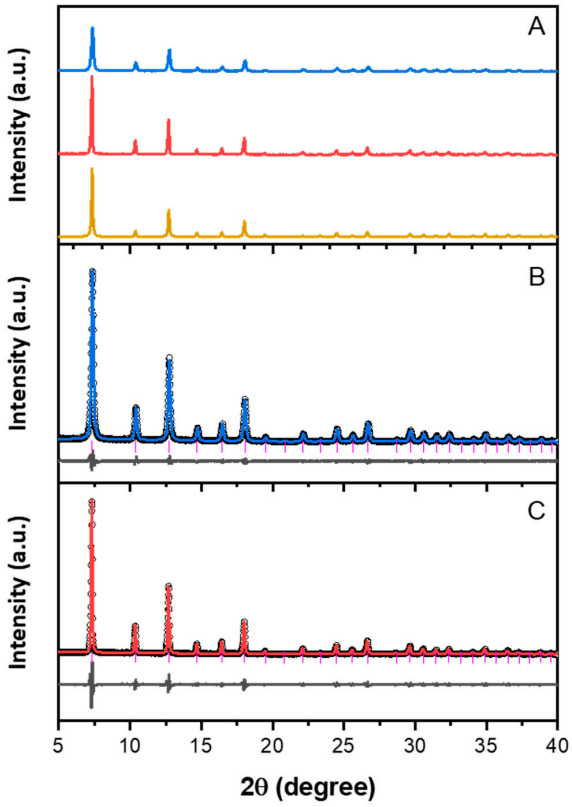

Figure 1. XRD patterns of (**A**) simulated reference ZIF-8 MOF spectra (yellow), measure ZIF-8 (blue) and measured ZIF-8-HT (red). Fitting of the XRD patterns of (**B**) ZIF-8 and (**C**) ZIF-8-HT. The blue and red lines are the fitted profile for ZIF-8 and ZIF8-HT, respectively. The black circles are the observed data, and the gray line is the difference in the two patterns. The ticks represent positions of allowed Bragg peaks for ZIF-8 MOF.

Table 1. Crystallographic parameters obtained by powder XRD analysis.

Catalyst	FWHM [1] (Degrees)	a (Å)	Volume (Å^3)	d (nm)
ZIF-8	0.20	17.0288(5)	4937.9(5)	34.9 ± 4.8
ZIF-8-HT	0.14	17.0500(3)	4956.5(3)	45.2 ± 11.4

[1] Full width half maximum values obtained from the XRD peak at 7.3°; a—lattice parameter obtained from fitting of the high resolution XRD data; d—crystal size obtained from Sherrer's analysis.

These crystal structures were further studied using FTIR spectroscopy. As shown in Figure 2, the spectra of both catalysts are in agreement with that of ZIF-8 in literature [39]. The peak at 422 cm^{-1} is the Zn–N stretch mode, which was observed at the beginning of the IR range available in our IR equipment. The majority of the absorption bands are associated with the vibrations of the imidazole units in the ZIF-8 framework. The bands below 800 cm^{-1} can be assigned as out-of-plane bending of the imidazole ring while those in the region of 900–1350 cm^{-1} are due to the in-plane bending. The bands between 1350 cm^{-1} and 1500 cm^{-1} can be assigned to the stretching of the entire ring, whereas the peak at 1584 cm^{-1} is due to the C=N stretch mode specifically. The bands at 2929 cm^{-1} and 3136 cm^{-1} are attributed to the aromatic and the aliphatic C–H stretch of the imidazole, respectively [40].

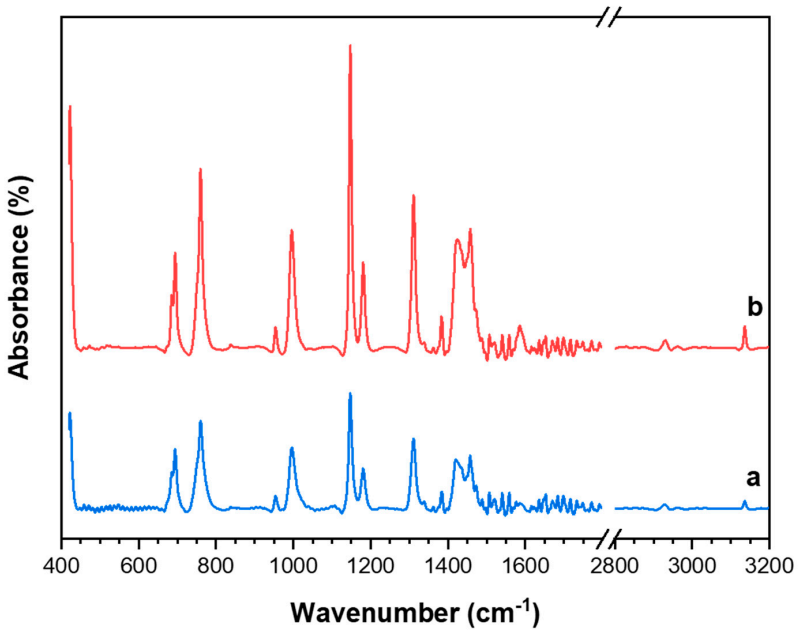

Figure 2. The FTIR spectra of (**a**) ZIF-8 and (**b**) ZIF-8-HT.

Thermogravimetric analysis was used to determine the thermal stability of the ZIF-8 materials. TGA plot of the catalysts are given in Figure 3A and the associated weight loss curves are shown in Figure 3B. TGA plot of the ZIF-8 catalyst revealed a ~1% weight loss starting at 210 °C up to 250 °C, which was attributed to the presence of the residual solvent or guest molecules. Similarly, the TGA plot of ZIF-8-HT shows a weight loss of ~3% between 200 °C and 250 °C. The decomposition of both samples occurred between 400 °C and 600 °C. The weight loss of the ZIF-8 dropped sharply at 400 °C, whereas the weight loss of ZIF-8-HT was smoother in the same temperature region. The remaining material resulting from ZnO after 600 °C for ZIF-8 and ZIF-8-HT are 34% and 37%, respectively. The TGA plots proved that both catalysts are thermally stable up to 400 °C, which is in line with previous literature reports [25].

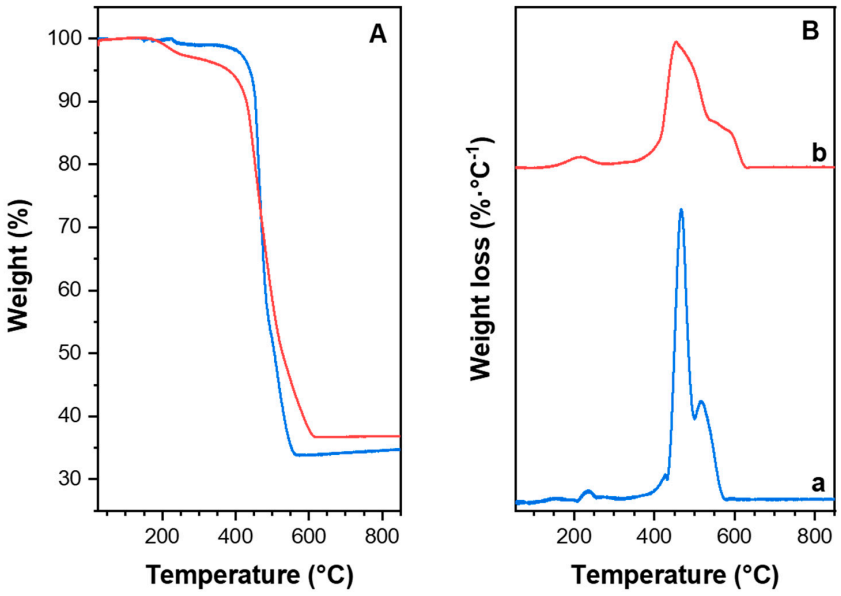

Figure 3. (**A**) Curves obtained from Thermal Gravimetric Analysis (TGA) measurements of ZIF-8 (blue line) and ZIF-8-HT (red line). (**B**) Weight loss curves from TGA measurements of (a) ZIF-8 and (b) ZIF-8-HT.

Nitrogen physisorption isotherms of the catalysts are shown in Figure 4. The textural properties derived thereof are summarised in Table 2. The isotherm of ZIF-8 is type I, which is indicative of a microporous material. For both materials a sharp increase are observed in the relative pressure range p/p_0 = 0.001–0.1 which indicates microporous structure. But, the ZIF-8-HT catalyst shows a type IV isotherm of mesoporous materials with a small H4 type hysteresis loop between relative pressures of 0.8 and 0.9. This points to the presence of slit-like mesopores, which can be understood as the interstitial mesopore voids between the adjacent MOF crystals. This is in line with the XRD analysis that the ZIF-8 material is less ordered than its hydrothermally synthesized ZIF-8-HT counterpart. The Brunauer–Emmett–Teller (BET) surface areas of ZIF-8 and ZIF-8-HT were calculated as 1351 $m^2 \cdot g^{-1}$ and 1967 $m^2 \cdot g^{-1}$, respectively, which are in line with earlier reports [41,42]. In particular, the ZIF-8-HT material has a notably high surface area closer to the theoretical value [25]. This indicates the highly crystalline nature of the ZIF-8-HT material. It is important to note that the applications of the BET equation to the physisorption data of the ZIF-8 materials reveal negative C values, thus the BET surface areas are treated as indicative hereby and they should be considered with care. The ZIF-8-HT catalyst shows only micropore volume (0.83 $cm^3 \cdot g^{-1}$), accompanied with negligible mesopore volume. Conversely, the ZIF-8 shows a lower micropore volume (0.54 $cm^3 \cdot g^{-1}$) than that of ZIF-8-HT.

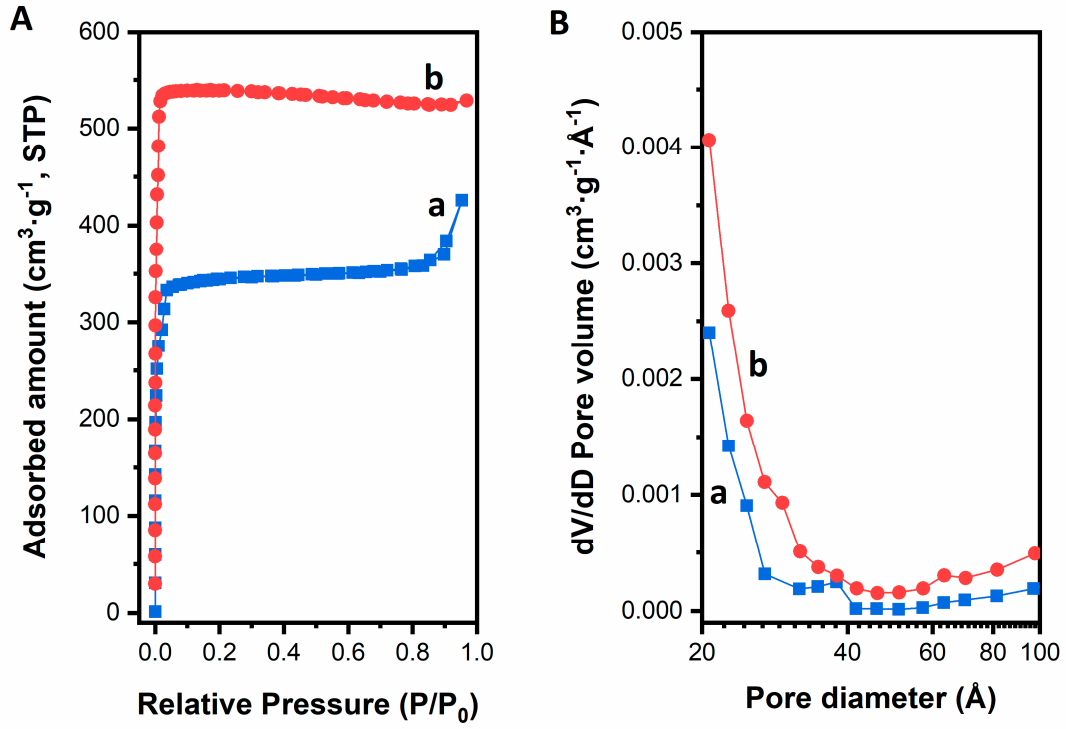

Figure 4. Nitrogen adsorption isotherms (**A**) and pore size distributions (**B**) of (**a**) ZIF-8 and (**b**) ZIF-8-HT measured at 77 K.

Table 2. Textural properties of the catalysts obtained from nitrogen adsorption analysis.

Catalyst	S_{BET} [1] ($m^2 \cdot g^{-1}$)	V_{Total} [2] ($cm^3 \cdot g^{-1}$)	V_{Meso} [3] ($cm^3 \cdot g^{-1}$)	V_{Micro} [4] ($cm^3 \cdot g^{-1}$)	Pore Size [5] (Å)
ZIF-8	1351	0.70	0.05	0.54	7.3
ZIF-8-HT	1967	0.83	-	0.83	6.6

[1] S_{BET} is the Brunauer–Emmett–Teller (BET) surface area obtained in the relative pressure range (p/p_0) of 0.001–0.20; [2] V_{Total} is the total pore volume at p/p_0 = 0.95; [3] V_{Meso} is the mesopore volume calculated from Barrett, Joyner, and Halenda (BJH) method; [4] V_{Micro} is the micropore volume calculated from *t*-plot method; [5] Pore size is the median pore width calculated by Horvath–Kawazoe method.

Scanning electron microscope (SEM) images of the ZIF-8 and ZIF-8-HT are shown in Figure 5. Both catalysts consists of large cubic shaped crystals. ZIF-8 catalyst has a broad distribution of crystal sizes in the range of 30–200 nm. The assembly of the crystals in ZIF-8 material infers the formation of intracrystalline voids, leading to the additional porosity observed in nitrogen physisorption studies. Conversely, the ZIF-8-HT has distinct crystals around 200 nm in size.

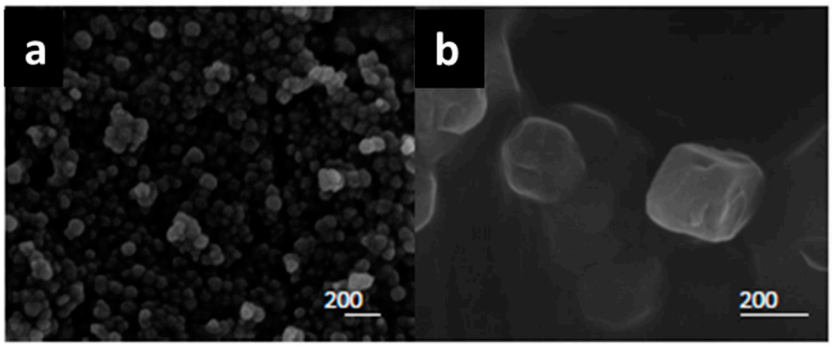

Figure 5. Scanning Electron Micrograph images of (**a**) ZIF-8 and (**b**) ZIF-8-HT. The scale bar represents 200 nm in each image.

2.2. Catalytic Activity

The ZIF-8 and ZIF-8-HT materials were tested as catalysts in the aqueous phase conversion of glucose for the production of HMF at 100 °C and 140 °C. The glucose conversion and yield of fructose, mannose, and HMF are tabulated in Table 3 and shown in Figure 6.

Table 3. Catalytic activity results under varying reaction conditions, with a 10 wt.% glucose aqueous stock solution.

Catalyst	pH [1]	Temperature (°C)	Glucose Conversion (%)	Fructose Yield (%)	Mannose Yield (%)	HMF Yield (%)
No catalyst	7.0	100	0.8	0.4	0	0
	7.0	140	5.6	0.8	0	2.1
	1.0	100	5.7	0	0	0.2
	1.0	140	18.4	0	0	4.2
$ZnCl_2$	7.0	100	5.6	2.6	0	0
	7.0	140	28.3	7.7	0.1	8.7
	1.0	100	5.5	0	0	0.2
	1.0	140	21.0	0	0	4.4
ZIF-8	7.0	100	25.3	15.3	0.3	0
	7.0	140	84.2	12.1	2.6	1.2
	1.0	100	11.9	5.4	0	0
	1.0	140	72.6	17.0	2.8	2.6
ZIF-8-HT	7.0	100	24.0	15.6	0.3	0
	7.0	140	82.3	12.1	2.6	1.2
	1.0	100	9.4	5.1	0	0
	1.0	140	74.4	16.7	3.0	2.2

[1] pH of 1 corresponds to an aqueous 0.1 M HCl solution.

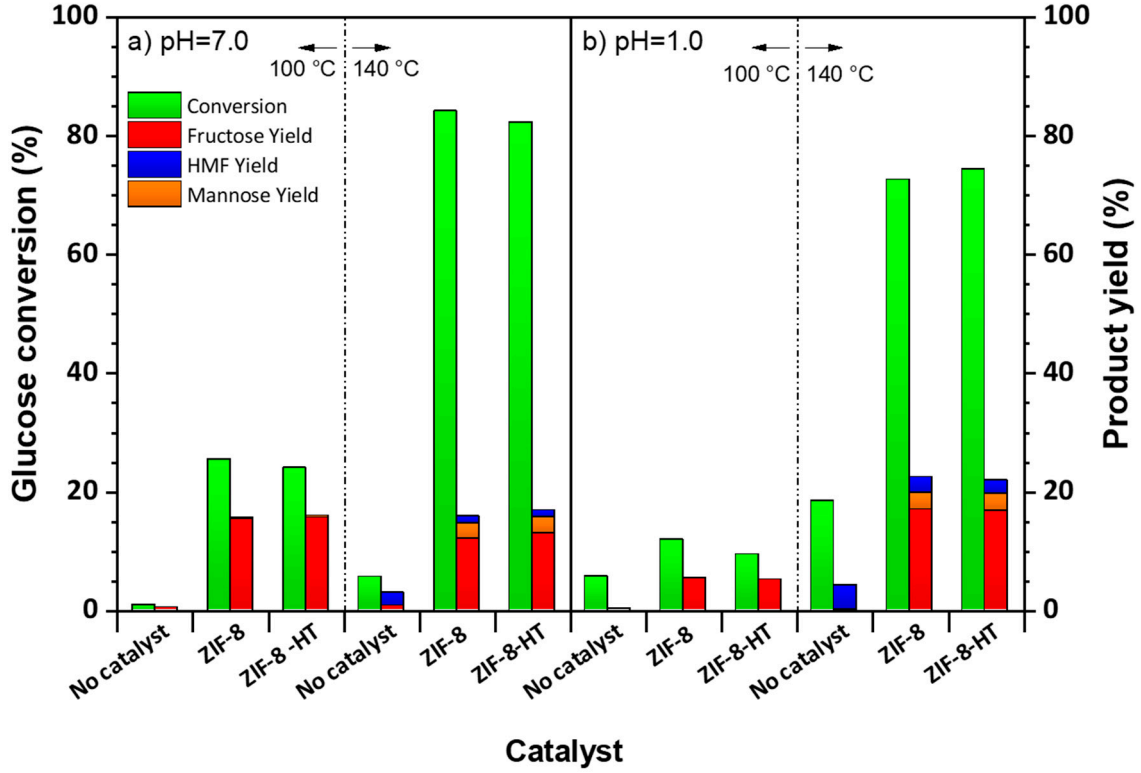

Figure 6. Glucose conversion and product yields at 100 °C and 140 °C in aqueous solutions at (**a**) pH = 7.0 and (**b**) pH = 1.0. Reactions were run in 3 mL batch reactors with 40 mg of catalyst starting with a 10 wt. % glucose in deionized water for 3h. pH = 1.0 corresponds to an aqueous 0.1 M HCl solution.

The conversion of glucose in the absence of any catalyst at 100 °C is negligible (Figure 6a, no catalyst). This is expected considering the stability and low reactivity of glucose in water. In the presence of ZIF-8, the glucose conversion increased to 25% and generate a total product yield of 15.6% corresponding to a 61.7% overall product selectivity. The results over ZIF-8-HT are similar with a slightly lower conversion (24%) and a similar overall product yield (15.9%). Both catalysts produce mainly fructose (>15%) and a small amount of mannose was observed (~0.4%). This suggests that Zn sites within the ZIF-8 framework exhibit sufficient Lewis acidity to promote glucose isomerisation. The Lewis acidity of ZIF-8 has previously been reported in literature and is specifically attributed to defective Zn sites with low coordination [43,44]. Furthermore, ZIF-8 is a hydrophobic framework [25,45]. Therefore the catalytic performance of ZIF-8 catalysts could also be attributed to its hydrophobic nature. Specifically, over the hydrophobic surface of ZIF-8 the competition between reactant and solvent molecules are in favour of the reactant, glucose. This is similar to the catalytic activity of Sn-Beta in glucose isomerisation [46,47]. The activity and selectivity of Sn-Beta is, in part, attributed to the hydrophobic nature of the Beta zeolite framework, which prevents the inhibition of active Sn sites by water molecules [48]. Glucose conversion over ZIF-8 and ZIF-8-HT catalysts at 140 °C are significantly higher (>80%) than the conversion at 100 °C, whereas the overall product yields remained similar at both temperatures. On the other hand, the product distributions are different for each temperature. In particular, larger quantities of mannose were produced at 140 °C. The temperature dependency of product distribution is evident by this result and this suggests that the higher temperatures enhance the epimerisation of glucose to mannose. We have performed the reactions also in the presence of zinc chloride (Table 3, $ZnCl_2$) with the same amount of Zn that ZIF-8 catalysts consists of. The conversion of glucose over the Zn itself revealed to be much lower than the ZIF-8 and ZIF-8-HT under the same conditions, and it is closer to the conversion without any catalyst. This indicates that Zn has limited activity in homogeneous phase.

The activity of the ZIF-8 and ZIF-8-HT catalysts were also tested at shorter reaction times (Figure 7). Both catalysts produced similar glucose conversions and product yields at 60 min. This is expected as the materials have the same structure and contain same quantities of organic linker and Zn, thus the number of active sites on both materials are expected to be similar. However, ZIF-8-HT has significantly higher surface area than ZIF-8. Despite this, ZIF-8 shows slightly higher activity at pH 7.0 and only slightly lower than ZIF-8-HT at pH 1.0 (Figure 6a,b at 140 °C, 3 h). This indicates that the higher surface area of ZIF-8-HT is beneficial at shorter reaction times (Figure 7), however it is not significantly different at longer reaction times (Figure 6). This implies that the reaction mainly occurs on the catalyst surface rather than the pores, where the latter requires the transport of bulky glucose molecule into the narrow pores of the MOF. The observed lower crystallinity of the ZIF-8 could lead to more defect sites (uncoordinated Zn centres) on its surface, which could enhance its activity in this reaction.

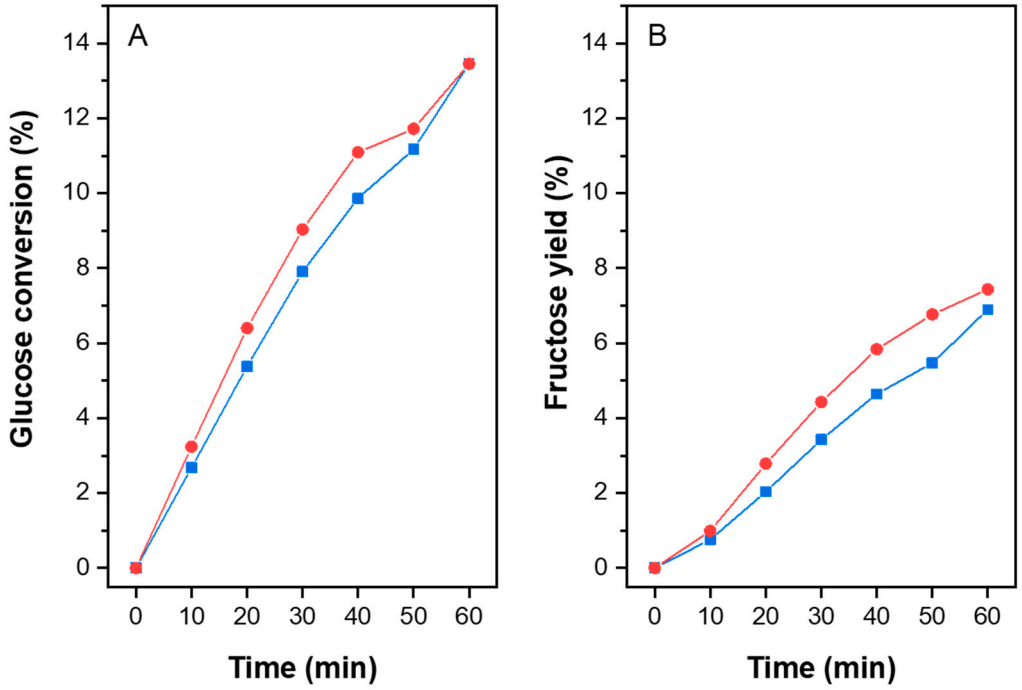

Figure 7. The results of the catalytic activity tests at 100 °C, at pH 7.0, in batch reactors for ZIF-8 (square) and ZIF-8-HT (circle) showing glucose conversion (**A**) and fructose yield (**B**). Yields of mannose and HMF are close to zero and therefore not included.

The quantities of HMF produced over both catalysts are remarkably low as compared to fructose. This is because the catalysts lack the Brønsted acidity which is needed to dehydrate fructose to form HMF. In order to increase the HMF yields by driving the reaction towards HMF, we performed catalytic activity tests at lower pH = 1.0 (0.1 M aqueous HCl solution). Figure 6b shows the catalytic activity tests at pH = 1.0. Slightly lower glucose conversions and product yields were obtained over both catalysts at lower pH, which is more significant at 100 °C than 140 °C. This shows that the addition of HCl hinders the performance of the catalysts. One reason could be that the chlorine ions introduced by the mineral acid swamps active Lewis acid sites within ZIF-8, resulting in lower glucose conversion. One interesting finding is that the main product is fructose. This indicates that the addition of the mineral acid does not effectively drive the reaction towards HMF particularly at 100 °C, which could be explained by the lower activity at this temperature. The addition of mineral acid increases glucose conversions and product yields at higher temperatures (i.e., 140 °C) more dramatically, resulting in slightly higher HMF yields. The difference between the glucose conversions at lower and higher pH values are less pronounced at higher temperatures. This indicates that the catalytic activity is more sensitive to the temperature than the pH.

In order to test the stability of the ZIF-8 catalyst, its catalytic performance was tested in a packed bed reactor. The performance of ZIF-8 is shown in Figure 8. The catalyst initially produces a glucose conversion of around 18%. From batch reactions (Figure 7), a glucose conversion of ~6% with a ~4% fructose yield was expected at this weight hourly space velocity (WHSV). It is anticipated that the high initial activity is due to the stabilisation of the catalytic bed. This high initial catalytic activity diminishes quickly with the increasing time on stream, ultimately resulting in a glucose conversion of around 2%. This indicates that the catalyst is either damaged during the reaction, or that the production of carbonaceous products (humins) quickly deactivates the catalyst. The formation of humins were previously reported over Sn-Beta crystal where it was indicated as the reason for catalyst deactivation [49].

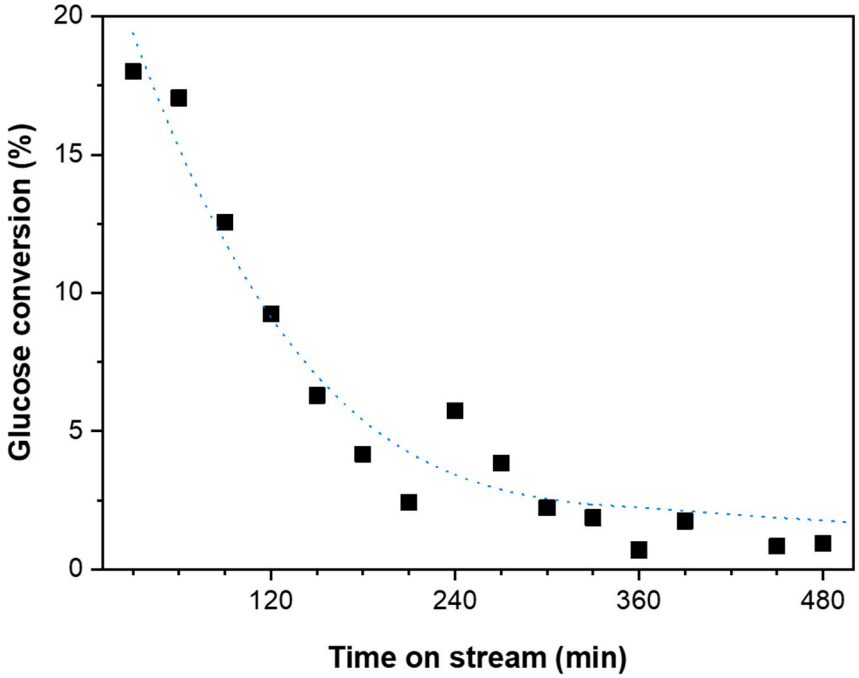

Figure 8. Catalytic activity of ZIF-8 in a continuous flow reactor at weight hourly space velocity (WHSV) of 10.5 h^{-1}.

3. Materials and Methods

Synthesis of ZIF-8 materials follows the typical synthesis procedures reported in literature [25]. Catalysts were synthesized by two methods. In the first method, all procedures were performed at room temperature (RT). First, 1.32 g (4.4 mmol) of zinc nitrate hexahydrate (99.0%, Honeywell, Seelze, Germany) was dissolved in 4 mL deionized water. Second, 11.37 g (138 mmol) of 2-methylimidazole (99%, Acros Organics, New Jersey, NJ, USA) was dissolved in 40 mL deionized water. Third, both solutions were mixed under rigorous mixing for 15 min. The final solution was then poured in centrifugal tubes and centrifuged at 6500 rpm for 30 min. The solid product was recovered and washed at least for four times with acetone. Finally, the product was dried in static oven for 24 h at 70 °C, and the catalyst is denoted as ZIF-8. In the second method, catalyst was prepared by hydrothermal (HT) synthesis method. First, 1.1 g (3.7 mmol) of zinc nitrate hexahydrate was dissolved in 5 mL deionized water. Next, 4.26 g (52 mmol) of 2-methylimidazole was dissolved in 15 mL deionized water. Then, both solutions were mixed under rigorous mixing for 15 min and transferred into a Teflon lined stainless steel autoclave (Parr Instruments, Moline, IL, USA). The autoclave was heated in oven at 140 °C for 24 h. Afterwards, the solution was recovered, and centrifuged at 6500 rpm for 15 min. The product was washed with acetone at least for four times. Finally, the product was dried in static oven for 24 h at 70 °C and denoted as ZIF-8-HT.

Powder XRD patterns were recorded on a X'Pert Pro MPD (Malvern Panalytical, Royston, UK), equipped with monochromatic Cu Kα_1 radiation (λ = 1.54056 Å) and 2θ = 2–40° (step size 0.015° in 2θ), operated at 40 kV and 40 mA. Profile fitting of the powder patterns was performed using the GSAS software (UChicago Argonne LLC, IL, USA, 2010) [50] implemented using the EXPGUI interface [51]. Nitrogen adsorption isotherms were collected in ASAP2020 (Micromeritics, Norcross, GA, USA) instrument at 77 K. All samples were degassed under vacuum at 120 °C for 8 h prior to measurements. Surface areas were calculated using the nitrogen adsorption between 0.001–0.2 p/p_0 via the Brunauer–Emmett–Teller (BET) method. Fourier Transform Infrared (FTIR) spectra were measured at room temperature in the range 400−4000 cm^{-1} using a Platinum-ATR Bruker Alfa instrument (Bruker Optics GmbH, Fällanden, Switzerland). The stability of the catalysts was investigated by TGA using a TGA/DSC1 instrument (Mettler Toledo, Columbus, Ohio, OH, USA) under ambient air pressure and a heating rate of 10 °C·min^{-1}. Samples were heated in air from 25 °C to 900 °C. Scanning electron microscopy (SEM) images of the catalysts were collected by a FEI SEM (FEI, Hillsboro, Oregon, OR, USA).

Catalytic screening was carried out in 4 mL batch reactors at 100 °C or 140 °C. 3 mL of 10 wt.% glucose solution was heated to the desired temperature together with the catalyst and a magnetic stirring bar (40 mg, corresponding to a 7.5 substrate to catalyst ratio, respectively) for 3 h. Blank experiments were also carried out without catalyst. The products were analysed by high performance liquid chromatography (HPLC) equipped with a Bio-Rad HPX 87P column (Shimadzu, Kyoto, Japan); a photo diode array detector and evaporative light scattering detector (ELSD) were used to monitor 5-HMF and sugars, respectively. The mobile phase was water with 0.6 mL·min^{-1} flow rate. The products and the reactant were quantified by calibration with external standards. The activity of catalysts under continuous flow was determined using a reactor system built in-house. An HPLC pump (Shimadzu LC-20AT, Kyoto, Japan) was used to pump the stock solution through a stainless steel tubular reactor (4.1 mm ID) which is capable of heating up to 400 °C, with a Eurotherm 3216 PID temperature controller (Schneider Electric, Rueil-Malmaison, France). At the exit of the reactor a Peltier module was used to cool the liquid leaving the reactor. Pressure within the system was controlled by a manual backpressure valve (Swagelok, Solon, Ohio, OH, USA) located downstream of the cooler. Sampling of the reaction mixture was achieved using a 10-port sample collection valve (Vici EUHA) which can be programmed for interval timing. Prior to each reaction, the catalyst were sieved (400 microns) and loaded to the reactor in between inert glass wool. At the inlet of the reactor, inert glass beads were packed to serve as preconditioning of the inlet flow. In a typical test, 80 mg of catalyst was pelletized and sieved to give a uniform particle size of ~250 μm. The catalyst was then mixed an inert material (silicon carbide) and loaded into the reactor resulting in a bed length of 8 cm. A 10 wt.% glucose solution in water was then continuously pumped through the reactor at a flow rate of 0.14 mL/min resulting in a weight hourly space velocity of 10.5 h^{-1}. Meanwhile, the reactor was heated to a desired reaction temperature. Samples were collected at the exit of the reactor every 30 min. The reaction solution collected in sample vials were analysed by HPLC as described above.

4. Conclusions

In this study, we presented the effect of synthesis temperature on the preparation of ZIF-8 and the applicability of the material as a cheap and easy to prepare alternative catalyst in the catalytic conversion of glucose to fructose and HMF. ZIF-8 has been synthesized using two different methods. Of these, the hydrothermal synthesis method yields a highly crystalline material with exceptionally high surface area. The synthesized materials were tested as catalysts for the isomerization of glucose and production of HMF. The materials showed activity in the glucose to fructose isomerization in batch reaction at a relatively low reaction temperature of 100 °C. Both ZIF-8 catalysts produced similar glucose conversions and product yields in water. The main product was fructose, which indicates that ZIF-8 exhibits Lewis acidity to promote glucose isomerization in water. Higher temperatures increased the conversion, however, it reduces the reaction selectivity for desirable products. Furthermore, higher

reaction temperatures promote glucose epimerization towards mannose. Conversely, in highly acidic conditions (0.1 M HCl), the activity of ZIF-8 was reduced at lower reaction temperatures and HMF production was slightly enhanced at higher temperatures. The activity of ZIF-8 in the flow reactor was initially high as expected, but it quickly diminished. This was either due to catalyst decomposition or deactivation caused by insoluble humins on the MOF surface. The activity of ZIF-8 halved in the flow reactor at 100 °C in 2.5 h, which implies that further studies are required to understand the deactivation mechanism and improve the long term hydrothermal stability of ZIF-8 materials under catalytic conditions in aqueous reaction medium. Understanding of reaction kinetics and humin formation will help to reveal the structure-activity relations of the catalysts to improve the long term catalyst stability.

Author Contributions: Conceptualization, V.D.; Formal analysis, R.O., S.D.K.R., and D.L.B.; Funding acquisition, V.D.; Investigation, R.O., S.D.K.R., and D.L.B.; Methodology, R.O., S.D.K.R., and D.L.B.; Supervision, C.H.L.T. and V.D.; Writing—original draft, V.D.; Writing—review & editing, C.H.L.T. and V.D.

Funding: This research was funded by the UK Engineering and Physical Sciences Research Council (EPSRC) [grant EP/P511432/1], Global Challenge Research Fund (GCRF) Institutional Award for the University of Warwick and the APC was funded by the University of Warwick. The data supporting this article are available at https://wrap.warwick.ac.uk/.

Conflicts of Interest: The authors declare no conflict of interest.

References

1. Wheeldon, I.; Christopher, P.; Blanch, H. Integration of heterogeneous and biochemical catalysis for production of fuels and chemicals from biomass. *Curr. Opin. Biotechnol.* **2017**, *45*, 127–135. [CrossRef] [PubMed]
2. Kang, S.; Fu, J.; Zhang, G. From lignocellulosic biomass to levulinic acid: A review on acid-catalyzed hydrolysis. *Renew. Sustain. Energy Rev.* **2018**, *94*, 340–362. [CrossRef]
3. Romo, J.E.; Bollar, N.V.; Zimmermann, C.J.; Wettstein, S.G. Conversion of Sugars and Biomass to Furans Using Heterogeneous Catalysts in Biphasic Solvent Systems. *ChemCatChem* **2018**, *10*, 4805–4816. [CrossRef] [PubMed]
4. Yavuz, E.; Cherkasov, N.; Degirmenci, V. Acid and base catalysed reactions in one pot with site-isolated polyHIPE catalysts. *RSC Adv.* **2019**, *9*, 8175–8183. [CrossRef]
5. Zhao, H.; Holladay, J.E.; Brown, H.; Zhang, Z.C. Metal Chlorides in Ionic Liquid Solvents Convert Sugars to 5-Hydroxymethylfurfural. *Science* **2007**, *316*, 1597–1600. [CrossRef] [PubMed]
6. Pidko, E.A.; Degirmenci, V.; van Santen, R.A.; Hensen, E.J.M. Glucose Activation by Transient Cr^{2+} Dimers. *Angew. Chem. Int. Ed.* **2010**, *49*, 2530–2534. [CrossRef] [PubMed]
7. Pidko, E.A.; Degirmenci, V.; Hensen, E.J.M. On the Mechanism of Lewis Acid Catalyzed Glucose Transformations in Ionic Liquids. *ChemCatChem* **2012**, *4*, 1263–1271. [CrossRef]
8. Pidko, E.A.; Degirmenci, V.; van Santen, R.A.; Hensen, E.J.M. Coordination Properties of Ionic Liquid-Mediated Chromium(II) and Copper(II) Chlorides and Their Complexes with Glucose. *Inorg. Chem.* **2010**, *49*, 10081–10091. [CrossRef]
9. Degirmenci, V.; Hensen, E.J.M. Development of a Heterogeneous Catalyst for Lignocellulosic Biomass Conversion: Glucose Dehydration by Metal Chlorides in a Silica-Supported Ionic Liquid Layer. *Environ. Prog. Sustain. Energy* **2014**, *33*, 657–662. [CrossRef]
10. Degirmenci, V.; Pidko, E.A.; Magusin, P.C.M.M.; Hensen, E.J.M. Towards a Selective Heterogeneous Catalyst for Glucose Dehydration to 5-Hydroxymethylfurfural in Water: CrCl2 Catalysis in a Thin Immobilized Ionic Liquid Layer. *ChemCatChem* **2011**, *3*, 969–972. [CrossRef]
11. Davis, M.E. Heterogeneous Catalysis for the Conversion of Sugars into Polymers. *Top. Catal.* **2015**, *58*, 405–409. [CrossRef]
12. Moliner, M.; Román-Leshkov, Y.; Davis, M.E. Tin-containing zeolites are highly active catalysts for the isomerization of glucose in water. *Proc. Natl. Acad. Sci. USA* **2010**, *107*, 6164–6168. [CrossRef] [PubMed]
13. Rajabbeigi, N.; Torres, A.I.; Lew, C.M.; Elyassi, B.; Ren, L.; Wang, Z.; Je Cho, H.; Fan, W.; Daoutidis, P.; Tsapatsis, M. On the kinetics of the isomerization of glucose to fructose using Sn-Beta. *Chem. Eng. Sci.* **2014**, *116*, 235–242. [CrossRef]

14. Toftgaard Pedersen, A.; Ringborg, R.; Grotkjær, T.; Pedersen, S.; Woodley, J.M. Synthesis of 5-hydroxymethylfurfural (HMF) by acid catalyzed dehydration of glucose–fructose mixtures. *Chem. Eng. J.* **2015**, *273*, 455–464. [CrossRef]
15. Román-Leshkov, Y.; Davis, M.E. Activation of Carbonyl-Containing Molecules with Solid Lewis Acids in Aqueous Media. *ACS Catal.* **2011**, *1*, 1566–1580. [CrossRef]
16. Gounder, R.; Davis, M.E. Monosaccharide and disaccharide isomerization over Lewis acid sites in hydrophobic and hydrophilic molecular sieves. *J. Catal.* **2013**, *308*, 176–188. [CrossRef]
17. Caratzoulas, S.; Davis, M.E.; Gorte, R.J.; Gounder, R.; Lobo, R.F.; Nikolakis, V.; Sandler, S.I.; Snyder, M.A.; Tsapatsis, M.; Vlachos, D.G. Challenges of and Insights into Acid-Catalyzed Transformations of Sugars. *J. Phys. Chem. C* **2014**, *118*, 22815–22833. [CrossRef]
18. Román-Leshkov, Y.; Moliner, M.; Labinger, J.A.; Davis, M.E. Mechanism of Glucose Isomerization Using a Solid Lewis Acid Catalyst in Water. *Angew. Chem. Int. Ed.* **2010**, *49*, 8954–8957. [CrossRef]
19. Rai, N.; Caratzoulas, S.; Vlachos, D.G. Role of Silanol Group in Sn-Beta Zeolite for Glucose Isomerization and Epimerization Reactions. *ACS Catal.* **2013**, *3*, 2294–2298. [CrossRef]
20. Osmundsen, C.M.; Holm, M.S.; Dahl, S.; Taarning, E. Tin-containing silicates: Structure-activity relations. *Proc. R. Soc. A* **2012**, *468*, 2000–2016. [CrossRef]
21. Zhang, Y.; Degirmenci, V.; Li, C.; Hensen, E.J.M. Phosphotungstic Acid Encapsulated in Metal-Organic Framework as Catalysts for Carbohydrate Dehydration to 5-Hydroxymethylfurfural. *ChemSusChem* **2011**, *4*, 59–64. [CrossRef] [PubMed]
22. Pertiwi, R.; Oozeerally, R.; Burnett, D.L.; Chamberlain, T.W.; Cherkasov, N.; Walker, M.; Kashtiban, R.J.; Krisnandi, Y.K.; Degirmenci, V.; Walton, R.I. Replacement of Chromium by Non-Toxic Metals in Lewis-Acid MOFs: Assessment of Stability as Glucose Conversion Catalysts. *Catalysts* **2019**, *9*, 437. [CrossRef]
23. Oozeerally, R.; Burnett, D.L.; Chamberlain, T.W.; Walton, R.I.; Degirmenci, V. Exceptionally Efficient and Recyclable Heterogeneous Metal–Organic Framework Catalyst for Glucose Isomerization in Water. *ChemCatChem* **2018**, *10*, 706–709. [CrossRef] [PubMed]
24. Lai, Z. Development of ZIF-8 membranes: Opportunities and challenges for commercial applications. *Curr. Opin. Chem. Eng.* **2018**, *20*, 78–85. [CrossRef]
25. Park, K.S.; Ni, Z.; Côté, A.P.; Choi, J.Y.; Huang, R.; Uribe-Romo, F.J.; Chae, H.K.; O'Keeffe, M.; Yaghi, O.M. Exceptional chemical and thermal stability of zeolitic imidazolate frameworks. *Proc. Natl. Acad. Sci. USA* **2006**, *103*, 10186–10191. [CrossRef] [PubMed]
26. Phan, A.; Doonan, C.J.; Uribe-Romo, F.J.; Knobler, C.B.; O'Keeffe, M.; Yaghi, O.M. Synthesis, Structure, and Carbon Dioxide Capture Properties of Zeolitic Imidazolate Frameworks. *Acc. Chem. Res.* **2010**, *43*, 58–67. [CrossRef]
27. Kolmykov, O.; Chebbat, N.; Commenge, J.M.; Medjahdi, G.; Schneider, R. ZIF-8 nanoparticles as an efficient and reusable catalyst for the Knoevenagel synthesis of cyanoacrylates and 3-cyanocoumarins. *Tetrahedron Lett.* **2016**, *57*, 5885–5888. [CrossRef]
28. Sun, C.Y.; Qin, C.; Wang, X.L.; Yang, G.S.; Shao, K.Z.; Lan, Y.Q.; Su, Z.M.; Huang, P.; Wang, C.G.; Wang, E.B. Zeolitic imidazolate framework-8 as efficient pH-sensitive drug delivery vehicle. *Dalton Trans.* **2012**, *41*, 6906–6909. [CrossRef]
29. Gong, X.; Wang, Y.; Kuang, T. ZIF-8-Based Membranes for Carbon Dioxide Capture and Separation. *ACS Sustain. Chem. Eng.* **2017**, *5*, 11204–11214. [CrossRef]
30. Xu, X.; Wang, H.; Liu, J.; Yan, H. The applications of zeolitic imidazolate framework-8 in electrical energy storage devices: A review. *J. Mater. Sci. Mater. Electron.* **2017**, *28*, 7532–7543. [CrossRef]
31. Li, J.; Wu, Y.N.; Li, Z.; Zhang, B.; Zhu, M.; Hu, X.; Zhang, Y.; Li, F. Zeolitic Imidazolate Framework-8 with High Efficiency in Trace Arsenate Adsorption and Removal from Water. *J. Phys. Chem. C* **2014**, *118*, 27382–27387. [CrossRef]
32. Bleith, T.; Deng, Q.H.; Wadepohl, H.; Gade, L.H. Radical Changes in Lewis Acid Catalysis: Matching Metal and Substrate. *Angew. Chem. Int. Ed.* **2016**, *55*, 7852–7856. [CrossRef] [PubMed]
33. Orazov, M.; Davis, M.E. Catalysis by framework zinc in silica-based molecular sieves. *Chem. Sci.* **2016**, *7*, 2264–2274. [CrossRef] [PubMed]
34. Zheng, B.; Sant, M.; Demontis, P.; Suffritti, G.B. Force Field for Molecular Dynamics Computations in Flexible ZIF-8 Framework. *J. Phys. Chem. C* **2012**, *116*, 933–938. [CrossRef]

35. Moggach, S.A.; Bennett, T.D.; Cheetham, A.K. The Effect of Pressure on ZIF-8: Increasing Pore Size with Pressure and the Formation of a High-Pressure Phase at 1.47 GPa. *Angew. Chem. Int. Ed.* **2009**, *48*, 7087–7089. [CrossRef] [PubMed]
36. Zhou, W.; Wu, H.; Udovic, T.J.; Rush, J.J.; Yildirim, T. Quasi-Free Methyl Rotation in Zeolitic Imidazolate Framework-8. *J. Phys. Chem. A* **2008**, *112*, 12602–12606. [CrossRef] [PubMed]
37. Liédana, N.; Galve, A.; Rubio, C.; Téllez, C.; Coronas, J. CAF@ZIF-8: One-Step Encapsulation of Caffeine in MOF. *ACS Appl. Mater. Interfaces* **2012**, *4*, 5016–5021. [CrossRef] [PubMed]
38. Haldoupis, E.; Watanabe, T.; Nair, S.; Sholl, D.S. Quantifying Large Effects of Framework Flexibility on Diffusion in MOFs: CH_4 and CO_2 in ZIF-8. *ChemPhysChem* **2012**, *13*, 3449–3452. [CrossRef]
39. Hu, Y.; Kazemian, H.; Rohani, S.; Huang, Y.; Song, Y. In situ high pressure study of ZIF-8 by FTIR spectroscopy. *Chem. Commun.* **2011**, *47*, 12694–12696. [CrossRef]
40. Ordoñez, M.J.C.; Balkus, K.J.; Ferraris, J.P.; Musselman, I.H. Molecular sieving realized with ZIF-8/Matrimid® mixed-matrix membranes. *J. Membr. Sci.* **2010**, *361*, 28–37. [CrossRef]
41. Butova, V.V.; Budnyk, A.P.; Bulanova, E.A.; Lamberti, C.; Soldatov, A.V. Hydrothermal synthesis of high surface area ZIF-8 with minimal use of TEA. *Solid State Sci.* **2017**, *69*, 13–21. [CrossRef]
42. Munn, A.S.; Dunne, P.W.; Tang, S.V.Y.; Lester, E.H. Large-scale continuous hydrothermal production and activation of ZIF-8. *Chem. Commun.* **2015**, *51*, 12811–12814. [CrossRef] [PubMed]
43. Zhu, M.; Srinivas, D.; Bhogeswararao, S.; Ratnasamy, P.; Carreon, M.A. Catalytic activity of ZIF-8 in the synthesis of styrene carbonate from CO2 and styrene oxide. *Catal. Commun.* **2013**, *32*, 36–40. [CrossRef]
44. Chizallet, C.; Bats, N. External Surface of Zeolite Imidazolate Frameworks Viewed Ab Initio: Multifunctionality at the Organic−Inorganic Interface. *J. Phys. Chem. Lett.* **2010**, *1*, 349–353. [CrossRef]
45. Zhang, K.; Lively, R.P.; Zhang, C.; Koros, W.J.; Chance, R.R. Investigating the Intrinsic Ethanol/Water Separation Capability of ZIF-8: An Adsorption and Diffusion Study. *J. Phys. Chem. C* **2013**, *117*, 7214–7225. [CrossRef]
46. van der Graaff, W.N.P.; Tempelman, C.H.L.; Li, G.; Mezari, B.; Kosinov, N.; Pidko, E.A.; Hensen, E.J.M. Competitive Adsorption of Substrate and Solvent in Sn-Beta Zeolite During Sugar Isomerization. *ChemSusChem* **2016**, *9*, 3145–3149. [CrossRef] [PubMed]
47. van der Graaff, W.N.P.; Tempelman, C.H.L.; Pidko, E.A.; Hensen, E.J.M. Influence of pore topology on synthesis and reactivity of Sn-modified zeolite catalysts for carbohydrate conversions. *Catal. Sci. Technol.* **2017**, *7*, 3151–3162. [CrossRef]
48. Gounder, R.; Davis, M.E. Beyond shape selective catalysis with zeolites: Hydrophobic void spaces in zeolites enable catalysis in liquid water. *AlChE J.* **2013**, *59*, 3349–3358. [CrossRef]
49. van der Graaff, W.N.P.; Tempelman, C.H.L.; Hendriks, F.C.; Ruiz-Martinez, J.; Bals, S.; Weckhuysen, B.M.; Pidko, E.A.; Hensen, E.J.M. Deactivation of Sn-Beta during carbohydrate conversion. *Appl. Catal. A Gen.* **2018**, *564*, 113–122. [CrossRef]
50. Toby, B.H.; Von Dreele, R.B. GSAS-II: The genesis of a modern open-source all purpose crystallography software package. *J. Appl. Crystallogr.* **2013**, *46*, 544–549. [CrossRef]
51. Toby, B. EXPGUI, a graphical user interface for GSAS. *J. Appl. Crystallogr.* **2001**, *34*, 210–213. [CrossRef]